

**Measuring of mass and spin of Dark Matter particles at  
ILC/CLIC**

I. F. Ginzburg,  
Sobolev Inst. of Mathematics, SB RAS  
and Novosibirsk State University  
Novosibirsk, Russia

# Dark matter. Candidates

In many models Dark Matter (DM) consists of particles similar to those in SM. Discovery of such a candidate for Dark Matter particle (DMP) and measurement of its properties is one of the most important problems for colliders. The LHC program solves this problem for some specific DM models. At the LHC it is difficult to expect high precision in the DM mass measurement and model independent determination its spin.

The experiments at ILC/ CLIC allow to detect unambiguously the DMP candidate, to measure accurately its mass and spin for a wide class of DMP models.

## Main advantages of ILC

1. Well fixed 4-momentum of elementary initial state
2. Well fixed coupling constants dark/known particles ( $\equiv \gamma$  or  $Z$ ) – constants of EW theory

In the considered models (like MSSM or IDM – inert doublet model)

**I.** DMP  $D$  with mass  $M_D$  has a new conserved discrete quantum number, which I denote as D-parity. All known particles are  $D$ -even, while the DM particle is  $D$ -odd.

**II.** In addition to the neutral DMP  $D$ , another  $D$ -odd particles exist, a charged  $D^\pm$  and, perhaps, neutral  $D^A$ , with the same spin  $s_D = 0$  or  $1/2$  as  $D$  and with masses  $M_+$  and  $M_A$  larger than  $M_D$ .

The D-parity conservation ensures stability of the lightest  $D$ -odd particle and restricts possible decay modes of  $D^A$  and  $D^\pm$ .

**III.**  $D$ -particles interact with the SM particles only via the covariant derivative in the kinetic term of the Lagrangian – gauge interactions with the standard electroweak gauge couplings  $e$ ,  $g$  and  $g'$ :

$$D^+D^-\gamma, \quad D^+D^-Z, \quad D^+DW^-, \quad D^+D^AW^-, \quad D^ADZ.$$

The astrophysics and cosmology allow different values of  $M_D$ . The LEP results mean that  $M_+, M_A \geq 80$  GeV.

I assume, for definiteness,  $M_+ - M_D, M_A - M_D, |M_+ - M_A| \geq 10$  GeV.

All numerical examples below — for  $M_D = 50$  GeV.

All cross sections below are expressed via

$$\sigma_0 \equiv \sigma(e^+e^- \rightarrow \gamma \rightarrow \mu^+\mu^-) = \frac{4\pi\alpha^2}{3s}.$$

The anticipated annual luminosity  $\mathcal{L}$  for ILC corresponds  $\mathcal{L}\sigma_0 \sim 10^5$ .  
At  $E \sim 250$  GeV  $\sigma(e^+e^- \rightarrow all) \sim 10\sigma_0$ .

# Processes

We consider production of  $D$ -particles in the process

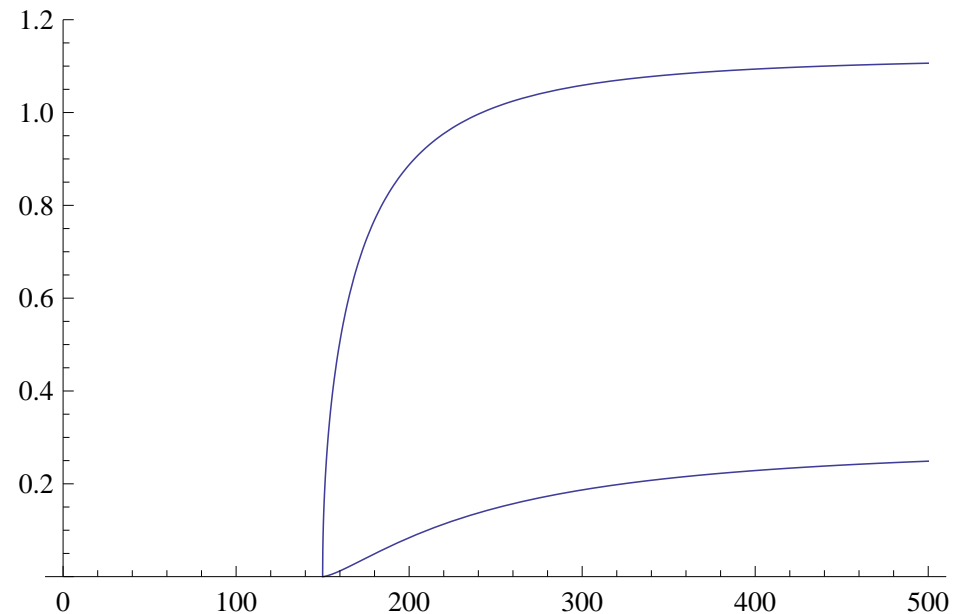
$$e^+e^- \rightarrow (\gamma, Z) \rightarrow D^+D^-,$$

+ subsequent decay of  $D^\pm \rightarrow DW^\pm$ , etc. with either on-shell or off-shell  $W$ 's and  $Z$ 's.

We assume that the ILC/ CLIC beam energy  $E = \sqrt{s}/2$  is sufficient, but the heavier  $D$ -particles, if they exist, cannot be produced.

The study of potential of process  $e^+e^- \rightarrow DD^A$  is more traditional. Its cross section is strongly model dependent, it is at least 4-6 times less at  $M_A \sim M_+$ .

The main part of  $\sigma(e^+e^- \rightarrow D^+D^-)$  is given by QED, at  $E > 100$  GeV model dependent  $Z$ -exchange contribute  $< 30\%$ .



$\sigma(e^+e^- \rightarrow D^+D^-)/\sigma_0$  at  $M_{\pm} = 120$  GeV vs beam energy  $E$ ,  
upper curve  $s_D = 1/2$ , lower curve  $s_D = 0$ .

# Signature

Observable states: (I) Decay products of  $W$ . (II) Large missing  $E_T - \cancel{E}_T$ , carried away by the neutral, stable  $D$ -particle + (III) *nothing*

$$e^+e^- \rightarrow D^+D^- \rightarrow DDW^+W^-$$

Two dijets or one dijet +  $e$  or  $\mu$  with large  $\cancel{E}_T$  + *nothing* with total energy for each dijet lower than  $E$ . The effective mass of each dijet is either  $M_W$  or lower than  $M_W$ . The missing mass  $M(\cancel{E}_T)$  is large. Typically these dijets (or dijet and lepton) move in the opposite hemispheres.

At  $M_A < M_+$  one more channel is added into the decay of  $D_{\pm}$ ,  
 $D_{\pm} \rightarrow D_A W^{\pm} \rightarrow DW^+W^-$ , with  $BR \leq 1/2$  and simple signature for  
 $e^+e^- \rightarrow D^+D^-$ .

(Reason for small BR: smaller final phase space in these decays in comparison with main decays at similar couplings)



Complete rate of processes with mentioned signature at known BR's gives  $\sigma(e^+e^- \rightarrow D^+D^-)$  with reasonable accuracy.

Measuring of singularities in the energy distribution of **lepton** in suitable fraction of these processes allow to determine masses  $M_+$  and  $M_D$ .

After that, **value of cross section will give us spin of  $D$ -particles  $s_D$** . (Measuring of end points in the energy distribution of di-leptons from  $Z$  in the process  $e^+e^- \rightarrow DD^A \rightarrow DDZ$  allow to determine masses  $M_A$  and  $M_D$ .)

# Energy distributions of products

- The produced in the process  $e^+e^- \rightarrow D^+D^-$  particles have the energy  $E_{\pm} = E$ , momentum  $p_{\pm} = \sqrt{E^2 - M_{\pm}^2}$ ,  $\gamma$ -factor  $\gamma_{\pm} = E/M_{\pm}$ , velocity  $\beta_{\pm} = p_{\pm}/E$ .
- The decay  $D^{\pm} \rightarrow DW^{\pm}$  in the rest frame is two-body decay with easily and unambiguously calculated parameters of produced  $W$ , energy  $E_W^r(M^*)$  and momentum  $p_W^r(M^*)$ . Here  $M^*$  is effective mass of decay products of  $W$ . For on-shell  $W$  we have  $M^* = M_W$ . For off shell  $W$  quantity  $M^*$  varies from 0 to  $M_{\pm} - M_D < M_W$ .
- The angular distributions of  $W$  in the rest frame of  $D^{\pm}$  is uniform (at least after averaging over intermediate spin state for spinor  $D$ -particles).

For off shell  $W$  at  $M^* \gtrsim 10$  GeV the branching ratios for different channels are roughly the same as for mass shell  $W$ .

To measure masses with reasonable precision, one can use only energy distributions of lepton from  $W$  in the process  $e^+e^- \rightarrow D^+D^- \rightarrow DDW^+W^- \rightarrow DD(q\bar{q})\mu\nu$  (events where the first  $W$  decays to  $\mu\nu$ , and the second one – to  $q\bar{q}$  (dijet).) The observable leptons from  $W$  decay don't represent  $W$  completely. The muon energy distribution is the convolution of energy distribution of  $W$  in the Lab system and distribution of  $\mu$  in the  $W$  rest frame.

At each fixed  $M^*$  possible energies of  $W$  in the lab system  $E_W^L$  are distributed within interval with end points  $E_{W\pm}^L$

$$E_{W+}^L = \gamma_{\pm}(E_W^r + \beta_{\pm}p_W^r) \geq E_W^L \geq E_{W-}^L = \gamma_{\pm}(E_W^r - \beta_{\pm}p_W^r); \quad (E_{W+}^L < E).$$

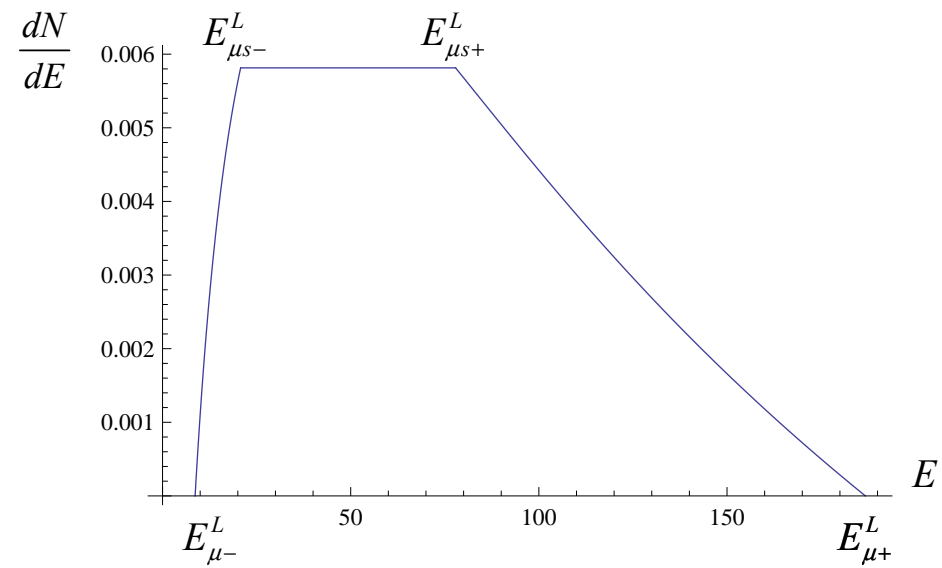
- **On shell  $W$ .** In the  $W$  rest frame energy and momentum of  $\mu$  are  $M_W/2$ . It is easy to find that the muon energies lie within the interval

$$E_{\mu+}^L \geq E_{\mu} \geq E_{\mu-}^L, \text{ where } E_{\mu\pm}^L = \frac{1}{2} \left( E_{W+}^L \pm \sqrt{(E_{W+}^L)^2 - M_W^2} \right).$$

Simple kinematical analysis shows that the total density of states within this interval increases monotonically from outer limits up to the energies

$$E_{\mu s\pm}^L = \frac{1}{2} \left( E_{W-}^L \pm \sqrt{(E_{W-}^L)^2 - M_W^2} \right).$$

Assumir  
frame c  
shari



$$M_{+} = 150 \text{ GeV}, M_D = 50 \text{ GeV}, E = 250 \text{ GeV}$$

- **Off shell  $W$**  has effective mass  $M^*$ , varying in the interval  $(0, M_+ - M_D)$ . At  $M^* \gtrsim 10$  GeV the distribution in  $M^*$  for each particular channel is given by the spin dependent factor  $R(s_D)dM^{*2}$ :

$$R(0) = \frac{(p_W^r(M^*))^3}{(M_W^2 - M^{*2})^2},$$

$$R(1/2) = \frac{\left[ 2(M_+^2 + M_D^2 - M^{*2}) - \frac{(M_+^2 + M_D^2)M^{*2} - (M_+^2 - M_D^2)^2}{M_W^2} \right] p_{Z^*}^r}{(M_W^2 - M^{*2})^2}.$$

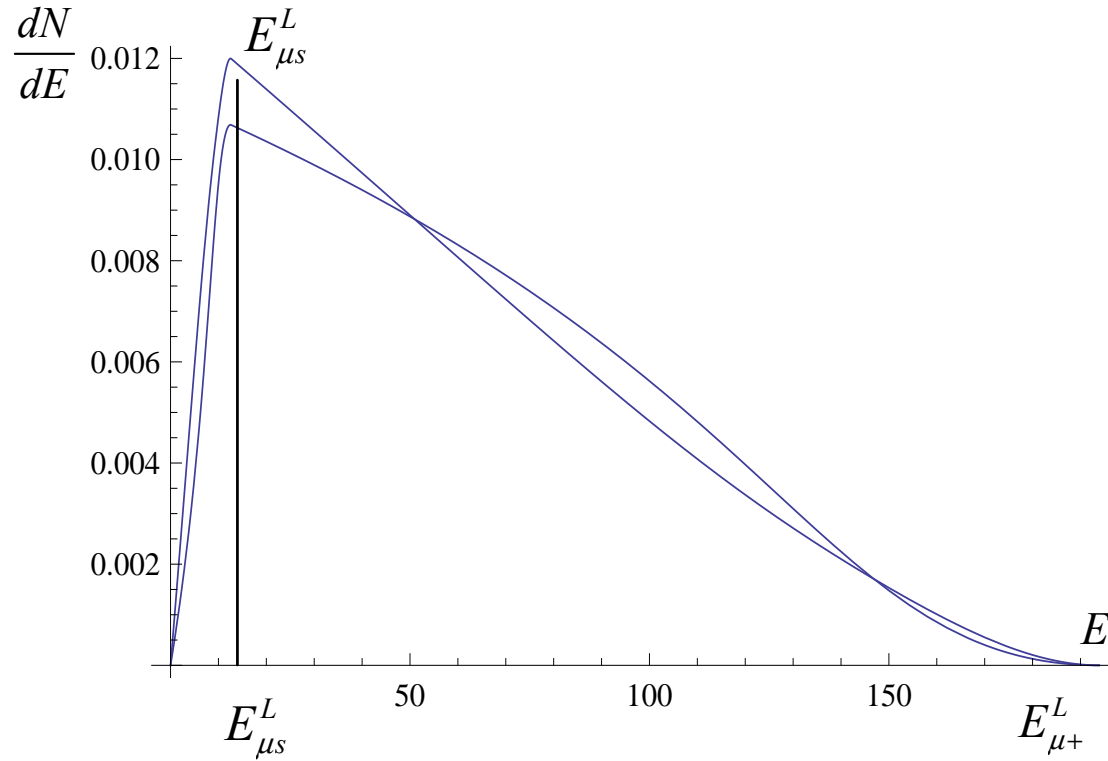
At each value  $M^*$  the energy distribution of muon is described by the same equation as for on shell  $W$  with the change  $M_W \rightarrow M^*$ . Complete energy distribution is obtained by integrated with weight  $R(s_D)dM^{*2}$ . As a result the muon energies lie within the interval

$$\left( 0, E_{\mu+}^L = \gamma_{\pm}(1 + \beta_{\pm}) \frac{M_+^2 - M_D^2}{2M_+} \right).$$

At the decreasing  $M^*$  position of kinks converge. Full energy distribution acquires a maximum, correspondent to  $M^* = 0$ , the density of states in muon energy has maximum at

$$E_{\mu s}^L = \gamma_{\pm}(1 + \beta_{\pm})(M_+ - M_D)/2.$$

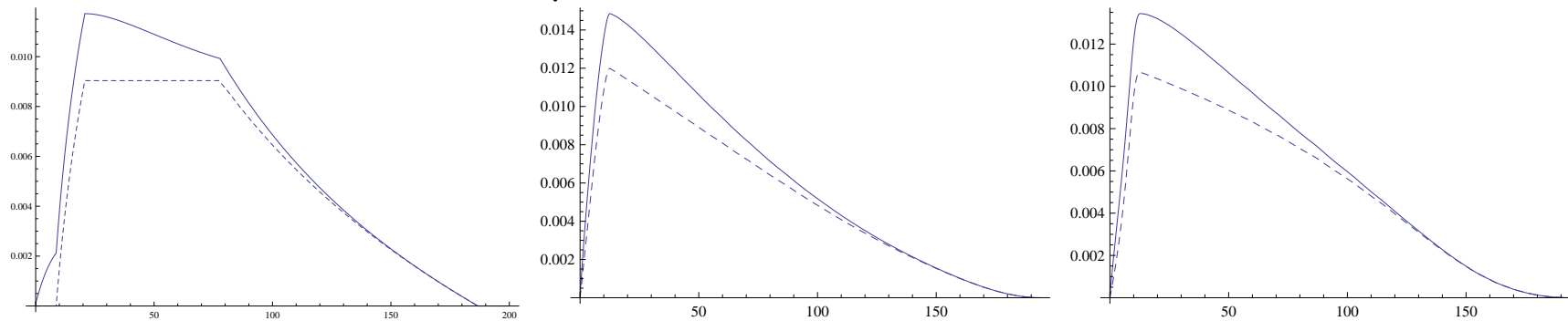
We see in figure sharp enough peak, which position don't depend on spin  $s_D$  and details of other distributions.



The energy distribution of single  $\mu$  from  $e^+e^- \rightarrow D^+D^- \rightarrow DDW^+W^-$  at  $M_+ = 120$  GeV,  $M_D = 50$  GeV,  $E = 250$  GeV. Upper peak corresponds  $s_D = 0$ , lower -  $s_D = 1/2$ .



The cascade decay  $D^- \rightarrow DW^- \rightarrow D\tau\bar{n}u \rightarrow D\mu\nu\bar{\nu}$  gives the same final state as that discussed above (adds 17% events). It is easy to understand that these muons are typically more slow than those from main process and influence weakly for singularities of spectrum. We calculated corrected spectra.



That are the same curves as above (dotted) with  $\tau \rightarrow \mu$  corrections. Positions of singularities are the same with accuracy better 1 GeV.

The formulas for end point  $E_{\mu+}^L$  and singular point  $E_{\mu s}L$  or  $E_{\mu s+}L$  provide two equations for finding two masses  $M_D$  and  $M_+$ .

The known values of  $M_+$  allow to calculate cross sections of processes  $e^+e^- \rightarrow D^+D^-$ . The results for spins  $s_D = 0$  and  $s_D = 1/2$  differ from each other by than 4 times  $\Rightarrow$  **Measured values of these cross sections give value of spin of DM  $s_D$ .**

**Backgrounds**– processes with the same observable state

either small or can be eliminated with suitable cuts.

Notation – our process – signal process (sig).

**BW1.**  $e^+e^- \rightarrow W^+W^-$ . Main differences.

(a)  $E_{BW1}(di - jet) = E$ , while  $E_{sig}(di - jet) < E$ ; (b) The missing mass  $M(\cancel{E}_T)_{BW1} = 0$ , while  $M(\cancel{E}_T)_{sig} = 0$  is large.

**BW2.**  $e^+e^- \rightarrow DD^A \rightarrow DDW^+W^-$  at  $M_A > M_+$ . If  $\sigma(e^+e^- \rightarrow DD^A)$  is not small at given  $\sqrt{s}$ , this fact will be seen via observation of process  $e^+e^- \rightarrow DDZ$ . The cross section  $\sigma(BW2) < \sigma(e^+e^- \rightarrow DDZ)$ , i.e. much less than  $\sigma(e^+e^- \rightarrow D^+D^- \rightarrow DDW^+W^-)$ . There are kinematical differences also.

**BW3.**  $e^+e^- \rightarrow D^+D^- \rightarrow DW^+D^AW^- \rightarrow DDW^+W^-Z_n$  at  $M_A < M_+$ .

Here  $Z_n$  is fraction of  $Z$  decaying to neutrinos. In this case the process  $e^+e^- \rightarrow DD^A$  is observable and the study of energy spectrum of dileptons in that process allows to determine masses  $M_A$  and  $M_D$ . Due to smaller phase space in decay  $D^\pm \rightarrow D^AW^\pm$ , the BR for latter decay less than 1/2. Therefore,  $\sigma(e^+e^- \rightarrow DDW^+W^-Z_n) = 0.2\sigma(e^+e^- \rightarrow DW^+D^AW^-) < 0.2\sigma(e^+e^- \rightarrow D^+D^- \rightarrow DW^+DW^-) \rightarrow$  the total fraction of these "incorrect" muons is less than 20% from the main process. The energy distribution of lepton in this process is described by the same equations as that for the signal process with natural replacement  $M_D$  to known  $M_A$ . Therefore, above distributions is transformed to the sum of two distributions of similar form with known  $M_D$ ,  $M_A$  and unknown  $M_+$ . Measuring singular points in this distribution allows to determine  $M_+$  and more precise value  $M_D$ .

**BW4.** In the other SM processes with observed state, satisfying our criterion, large  $E_T$  is carried away by additional neutrinos. The corresponding cross section is at least one electroweak coupling constant squared  $g^2/4\pi$  or  $g'^2/4\pi$  smaller than  $\sigma_0$ , with  $g^2/4\pi \sim g'^2/4\pi \sim \alpha$ . Therefore, the cross sections for these background processes are about one or two orders of magnitude smaller than the cross section of the process under discussion.

**The end**